Cell crawling mediates collective cell migration to close undamaged epithelial gaps

Ester Anon[a,b], Xavier Serra-Picamal[b], Pascal Hersen[a,c], Nils C. Gauthier[c], Michael P. Sheetz[c,d], Xavier Trepat[b,e,1], and Benoît Ladoux[a,c,1]

[a]Laboratoire Matière et Systèmes Complexes, Université Paris Diderot and Unité Mixte de Recherche 7057 Centre National de la Recherche Scientifique, F-75205 Paris Cedex 13, France; [b]Institute for Bioengineering of Catalonia, University of Barcelona and Ciber Enfermedades Respiratorias, 08036 Barcelona, Spain; [c]Mechanobiology Institute, National University of Singapore, Singapore 117411; [d]Department of Biological Sciences, Columbia University, New York, NY 11027; and [e]Institució Catalana de Recerca i Estudis Avançats, 08010 Barcelona, Spain

Edited by William M. Bement, University of Wisconsin, Madison, WI, and accepted by the Editorial Board May 11, 2012 (received for review October 29, 2011)

Fundamental biological processes such as morphogenesis and wound healing involve the closure of epithelial gaps. Epithelial gap closure is commonly attributed either to the purse-string contraction of an intercellular actomyosin cable or to active cell migration, but the relative contribution of these two mechanisms remains unknown. Here we present a model experiment to systematically study epithelial closure in the absence of cell injury. We developed a pillar stencil approach to create well-defined gaps in terms of size and shape within an epithelial cell monolayer. Upon pillar removal, cells actively respond to the newly accessible free space by extending lamellipodia and migrating into the gap. The decrease of gap area over time is strikingly linear and shows two different regimes depending on the size of the gap. In large gaps, closure is dominated by lamellipodium-mediated cell migration. By contrast, closure of gaps smaller than 20 μm was affected by cell density and progressed independently of Rac, myosin light chain kinase, and Rho kinase, suggesting a passive physical mechanism. By changing the shape of the gap, we observed that low-curvature areas favored the appearance of lamellipodia, promoting faster closure. Altogether, our results reveal that the closure of epithelial gaps in the absence of cell injury is governed by the collective migration of cells through the activation of lamellipodium protrusion.

epithelial cell migration | microfabrication | wound model assay | Madin-Darby canine kidney cells

A wide variety of processes in health and disease involve the formation and closure of epithelial gaps. In embryos, naturally occurring gaps appear at different stages of development as a consequence of morphogenetic movements (1). A paradigmatic example is the well-studied process of dorsal closure in *Drosophila*, whereby epithelial sheets migrate over the amnioserosa cell layer to seal an eye-shaped opening (2). In adults, gaps in epithelial barriers result from dynamic tissue homeostasis, as clearly illustrated by epithelial turnover in the intestine (3). Moreover, epithelial gaps are commonly formed during trauma and chronic inflammatory diseases in which the epithelium is injured and often completely denuded. A rapid healing of these gaps is crucial to restore a functional epithelium and to prevent further damage.

Because of the importance of the maintenance of epithelial functions and homeostasis, many efforts have been devoted to study gap closure, and two distinct mechanisms have emerged (4–7). One mechanism is based on the assembly and contraction of a multicellular acto-myosin belt lining the gap (known as purse-string) (8), which is controlled by RhoA and its direct regulators Rho kinase (ROCK) and myosin light chain kinase (MLCK) (9). With a purse-string closure, the driving force is thus provided by the contraction of the actomyosin cable around the wound (10, 11). The second mechanism is based on cell migration mediated by lamellipodial protrusion, which is mostly regulated by Rac1 GTPase (9). In such cases, the mechanics of the process seem less clear because the driving mechanism could be the pressure exerted by surrounding cells, the pulling force from leader cells, or both (6, 7, 12).

The intricacy of the process and its regulation by the complex family of Rho-GTPases has promoted the appearance of many studies providing opposing roles for the different regulators (5, 13, 14). Cell–cell junctions play also an important role in the process, because it has been suggested that the purse-string is anchored at adherens junctions (15) or at tight junctions (16). Ample evidence now supports each of these two mechanisms, but their relative contribution to gap closure remains uncertain.

The controversy is also fostered by the variability in the experimental conditions used to create the gaps. The most commonly used methods to create gaps within cell monolayers are either the classic scratch wound assay, in which a strip of cells is mechanically removed with a pipette tip or a razor blade (17), or laser ablation, in which single cells are destroyed by a laser pulse (5). Both techniques are difficult to standardize because the final size and shape of the gap depend either on the shape and velocity of the scratching utensil or on the power and focal plane of the laser. Moreover, damage of cells during the process of wound production releases a complex and poorly characterized mixture of signaling molecules, death factors, and cell debris that influence the mechanisms of closure (18, 19).

How the actomyosin cable and/or lamellipodial protrusions are activated during epithelial gap closure is unclear but may involve secretion of soluble factors and/or mechanical tension. Up to now, most of the literature is based on the study of wound closure, whereby wounds are created by an aggressive method that releases a complex and unknown mixture of debris and death factors (20, 21). The central question of epithelial gap closure is thus still controversial and has not been addressed using well-defined physical and geometrical conditions. To overcome these limitations, we present a unique strategy to induce well-defined gaps within an epithelial monolayer and monitor the dynamics of epithelial gap closure in the absence of cell injury.

Results and Discussion

Dynamics of Epithelial Closure After Pillar Removal. By using a stencil of poly-dimethylsiloxane (PDMS) micropillars (Fig. 1), we could obtain many gaps of well-defined size and shape (Fig. 1 *G–I* and Table S1). The size and shape of the pillars were varied to obtain circular pillars of different diameters, ranging from 15 to 150 μm, and squared and ellipsoidal pillars of two different sizes

Author contributions: E.A., M.P.S., X.T., and B.L. designed research; E.A., X.S.-P., X.T., and B.L. performed research; E.A., X.S.-P., P.H., N.C.G., M.P.S., X.T., and B.L. analyzed data; and E.A., X.T., and B.L. wrote the paper.

The authors declare no conflict of interest.

This article is a PNAS Direct Submission. W.M.B. is a guest editor invited by the Editorial Board.

Freely available online through the PNAS open access option.

[1]To whom correspondence may be addressed. E-mail: xtrepat@ub.edu or benoit.ladoux@univ-paris-diderot.fr.

This article contains supporting information online at www.pnas.org/lookup/suppl/doi:10.1073/pnas.1117814109/-/DCSupplemental.

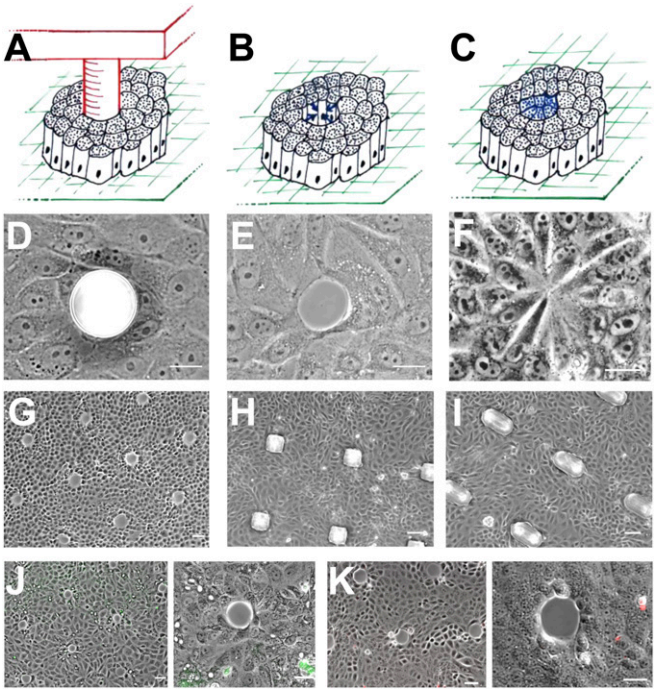

Fig. 1. Experimental design for gap patterning. (*A–C*) Schematic view of the approach used for the experimental model: (*A*) PDMS pillar surrounded by cells, (*B*) gap created upon pillar removal, (*C*) gap closed. (*D–F*) Phase-contrast micrographs of the different stages of the experimental model: (*D*) PDMS pillar surrounded by cells, (*E*) gap created upon pillar removal (note that the cells bordering the gap are intact), (*F*) gap closed by cells. (*G*) Array of gaps created by using a stencil with numerous PDMS pillars. (*H* and *I*) Microfabricated squared (*H*) and ellipsoidal (*I*) PDMS pillars with MDCK cells cultured within the pillar stencil. (*J*) Assessment of cell viability by FITC-dextran uptake. Note that none of the gap lining cells shows positive for FITC-dextran. (*K*) Assessment of cell viability by propidium iodide internalization. (Scale bars, 10 μm in *D–F*, 20 μm in *G–K*.)

(Fig. 1 *D*, *H*, and *I*). The PDMS pillars are coated with a non-adhesive polymer to prevent cell attachment and are surrounded by cells. In such a way, there are no specific adhesions between the pillars and the bordering cells, the pillar being a mere blocking object (Fig. S1 *A* and *B*). Madin-Darby canine kidney (MDCK) cells are cultured in between the pillars for 15 ± 3 h. Upon careful removal of the PDMS pillar, a gap is created within the monolayer, without tearing the bordering cells (Fig. 1 *E*, *G*, *J*, and *K*). Additionally, we performed scratch-induced gaps either by the removal of pillars on which cells were able to adhere (resulting in "ripped" gaps) or by pushing pillars against a preformed epithelial monolayer to kill the cells underneath (resulting in "crushed" gaps) (more details in *SI Materials and Methods*), to compare our model experiment with more classic scratch assays. We assessed cell damage by using FITC-dextran (22) as well as propidium iodide internalization by damaged cells. Both tests ascertained the absence of damage in our pillar removal assay, whereas they revealed cell damage in the case of ripped and crushed gaps and in the classic scratch assay (Fig. 1 *J* and *K* and Fig. S2 *A* and *B*). Thus, our methodology prevents the damage of cells surrounding the pillar after removal, as opposed to what is observed during classic scratch assays.

We first analyzed the dynamics of epithelial gap closure after removal of circular pillars of different diameters. Video microscopy experiments upon pillar stencil removal revealed that cells lining the gap extended lamellipodia throughout the process of closure (Fig. 2*A* and Movie S1). The borders of the gap roughened considerably after the removal of the pillar, indicating the extension of cellular protrusions into the available free space. We quantitatively analyzed the variations of the contour length by measuring the shape factor, $\alpha = \frac{2}{R}\frac{A}{p}$, which is the ratio of the area A over the contour length of the interface p normalized by half the instantaneous radius R. For a very rough interface, $\alpha \sim \mathbf{0}$, whereas $\alpha \sim \mathbf{1}$ for a perfectly circular hole. We indeed observed a decrease of this parameter α with time from 1 (at $t = 0$) down to approximately 0.6 as the boundary became irregular owing to the emergence of lamellipodium surrounding the gap (Fig. 2*B*).

According to previous studies, it was suggested that purse-string contraction repaired small epithelial wounds (4, 5), whereas larger wounds induced also cell crawling with formation of lamellipodia (6, 7, 23). Surprisingly, the presence of lamellipodia was observed for all gap sizes tested from 15 up to 150 μm (Movies S1 and S2). The formation of lamellipodia started shortly after the release of the PDMS pillar (during the first 10 min) and were present until there was no more available space, at which point opposing or contiguous lamellipodia contacted and fused. In small gaps (15–30 μm), all cells contacting the gap extended lamellipodia. For larger gaps, the number of cells at the gap border increased, and not all of these cells extended lamellipodia (Movie S2). Despite the presence of lamellipodia, the closure of gap was roughly isotropic, implying there was not the so-called fingering activity (24). We then sought to analyze the time evolution of the gap area, $A(t)$, during epithelial closure. In all conditions tested, the decrease of the area with time was strikingly linear with time down to a complete closure (Fig. 2*C* and Fig. S3*A*). The trend in the decrease of the gap area as function of time was similar for the different initial gap diameters, except for the smallest ones (for diameters of 15 and 20 μm). As shown on Fig. 2*D*, the closure time varied linearly with the size of the gap above a gap diameter of 20 μm. By analyzing the slope of $A(t)$, we computed the initial radial velocity (which represents the velocity at the onset of closure) as a function of the gap size and was found to be roughly constant (0.3 μm/min) for areas up to 750 μm^2 and then slightly decreased for larger gaps (Fig. 2*E*). Consistently, the advancement velocities of the protruding lamellipodia were found to be approximately 0.3 μm/min during the initial stage of lamellipodia formation (computed from the kymographs like Fig. S3*B*). Similarly, the cell body advancement displayed the same velocity at the onset of gap closure. Altogether, these results showed that the lamellipodium extension governed the kinetics of the mechanism of gap closure and suggested the possibility of a size-dependent mechanism in the dynamics of gap closure. As a comparison, we observed that the dynamics of damage-associated gaps exhibited broader distributions due to variable initial conditions and followed exponential decay laws as a function of time (Fig. S2*C*). This indicates that the presence of damaged cells or debris strongly altered the dynamics of epithelial gap closure. Interestingly, the closure dynamics of these "wounds" are consistent with reported data on embryonic wound healing and adult epithelial wound closure (15, 25).

To rule out an effect of differential extracellular matrix assembly that could provide directional cues to govern cell migration, we checked the status of the extracellular matrix (ECM) organization and secretion during our experiments (Fig. S4). Fibronectin was deposited on the substrate beneath the cells and the pillars. After removing the pillar, fibronectin was not affected, and cells migrated over this fibronectin substrate (Fig. S4 *A–D*). Moreover, the staining of the overall fibronectin due to the coating and cell secretion did not exhibit any specific pattern (Fig. S4*E*). Laminin was absent in the gap area but present in the cells as a synthetized protein, not structured in basal lamina yet (Fig. S4*G*). Throughout all of the experiments, because there was a fibronectin-based ECM roughly distributed everywhere onto the substrate, our observations could not be attributed to ECM remodeling underneath the monolayer as a driving mechanism.

We then analyzed the influence of cell culture density on the progression of closure. MDCK cells are epithelial cells that can undergo epithelial-to-mesenchymal transition (26). One could argue, therefore, that before pillar removal cells are already in a promigratory mesenchymal-like state, thus the protrusion of lamellipodia and active cell migration observed would not be a de novo response triggered by the sudden availability of free

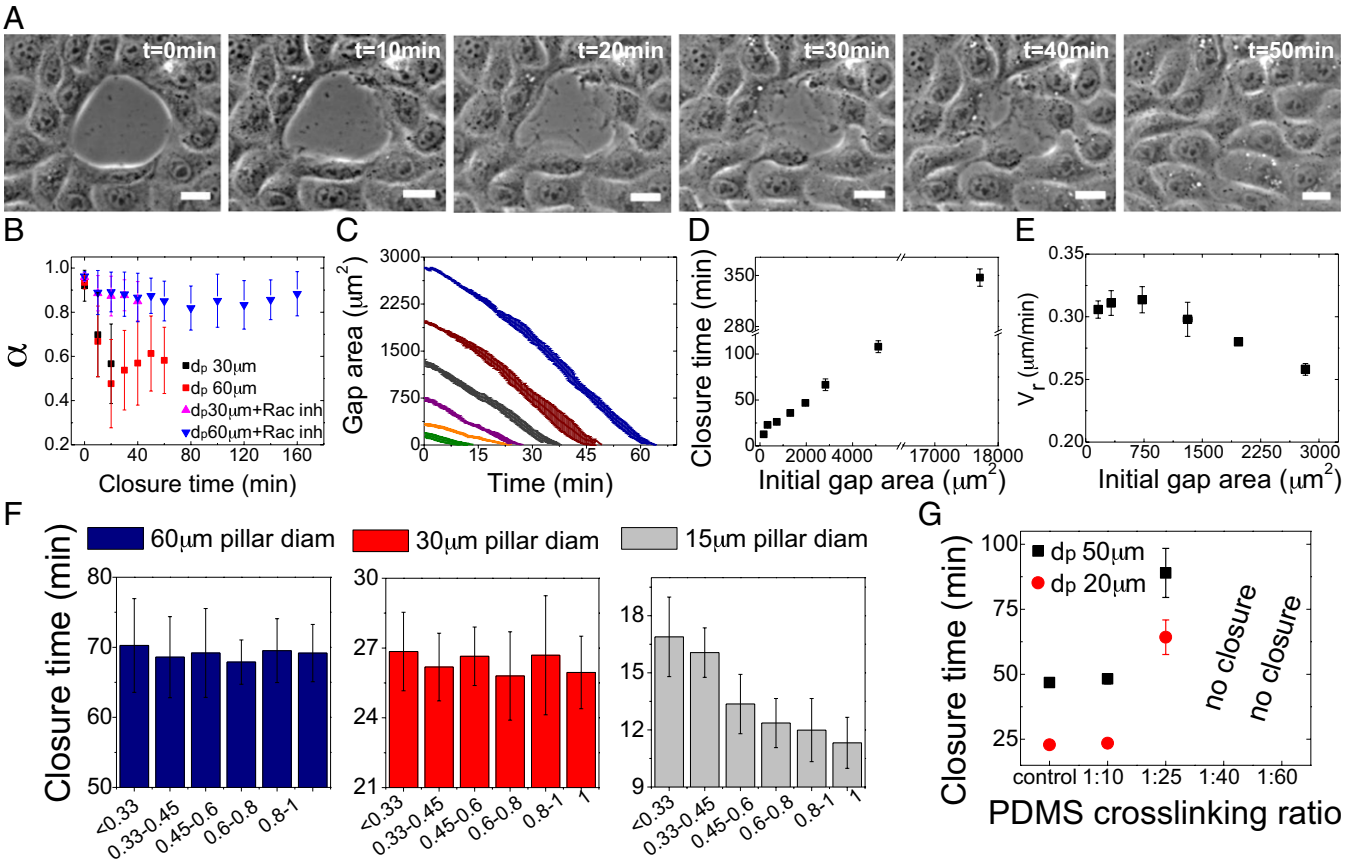

Fig. 2. Dynamics of gap closure. (*A*) Snapshots of time-lapse video microscopy during gap closure. $t = 0$ is acquired right after removal of the pillar stencil. (Scale bars, 20 μm.) (*B*) Evolution of roughness α at the cell–gap interface. Experiments performed with two pillar sizes, 30 and 60 μm in diameter. (*C*) Gap area decrease with time, for different pillar sizes used for creating the gaps, ranging from 15 to 60 μm in diameter. Green line corresponds to gaps created with pillars of 15 μm in diameter, orange 20, purple 30, black 40, red 50, and blue 60. Data for 80- and 150-μm pillar diameter are shown in Fig. S3. Data are reported as mean and SD of eight gaps analyzed per each size, resulting from four independent experiments. (*D*) Closure time as a function of the initial gap area of circular gaps. (*E*) Initial radial velocity depending on the initial gap size. (*F*) Effect of cell density on closure time, examined for three different gap diameters. Cell density is indicated in the x axis, calculated from Table S2. Each graph shows the experiments from a different pillar diameter. (*G*) Effect of substrate stiffness on the closure time of two different gap diameters, 20 and 50 μm. The *x* axis indicates the PDMS ratio used to attain different stiffnesses. *No closure* stands for gaps that were not closed after 300 min.

space. To rule out this possibility, we tested different cell packing densities, ranging from highly spread and flattened cells to the maximal density of cells within the culture, always after confluence was reached (Fig. S5 and Table S2). For large gaps (30- and 60-μm diameters), cell density had no impact either on the closure time or on protrusive activity (Fig. 2*F*). In addition, this result confirmed that the closure mechanism was not triggered by a possible release of the internal pressure within the epithelial cell sheet after the removal of the pillar but instead by the lamellipodium extension. However, for the smallest gaps, there was a decrease in the closure time as packing density increased, further suggesting that distinct mechanisms govern the closure of small vs. large gaps.

Force Generation on Stiff Substrates Induces Epithelial Gap Closure by Lamellipodium Activation. To verify that the activation of lamellipodium formation could be the driving force of cell migration into the gap, we tested the effects of the substrate rigidity on the dynamics of epithelial gap closure. Substrate stiffness is known to activate cell migration, to increase cell spreading and traction forces (27), and to govern lamellipodium dynamics (28). We observed MDCK cell migration after pillar removal on a PDMS substrate whose stiffness was tuned by changing the percentage of the reticulating agent (to 1:25, 1:40, and 1:60 PDMS cross-linker:base ratio; *SI Materials and Methods*), and we verified that the ECM coating was not affected within such a range of rigidities (Fig. S4*F*). Experiments performed on PDMS substrates of Young's modulus equivalent to glass (at 1:10, Young's modulus is 0.5–2 MPa) showed no differences either in dynamics or in closure time with respect to control experiments. As the stiffness decreased, we observed a drastic decrease of the migration speed of the cells into the gap (a 2.7-fold increase in closure time of 20-μm gaps and 1.9-fold in 50-μm gaps) (Fig. 2*G*). Furthermore, softer substrates (1:40 and 1:60) prevented the final closure of the gap even after 300 min, as well as the formation of lamellipodial protrusions (Movie S3). Therefore, stiff substrates were needed to generate the activation of the lamellipodium around the gap and stabilize it. Because cells are probing substrate stiffness by applying contractile forces (27, 29), it seems that the pulling force induced by leading cells that exhibited lamellipodial protrusions is a key player in our experimental model of epithelial closure.

Universal Mechanism Drives Closure of Small Gaps. Because the movement of epithelial cell sheets during wound closure could exhibit a purse-string mechanism, lamellipodium-based crawling, or both mechanisms simultaneously or at different stages (8, 23), we explored their relative contribution in our model experiment of epithelial gap closure. We tested the role of lamellipodial protrusion by inhibiting Rac1 and the role of the contractile machinery by inhibiting ROCK, MLCK, and myosin phosphorylation (Fig. S6). For each of these treatments and cell lines, we

measured the closure time as a function of the initial gap size. First, we observed that the closure time for small gaps (≤20 μm) was insensitive to all of the pharmacological treatments mentioned above for the inhibition of Rac or Rho pathways (Fig. 3*A*), further suggesting that a mechanism independent of the proposed regulators could induce the gap closure in such cases. According to the experimental results, two regimes emerged, depending on gap size. For small gaps (≤20 μm), we observed different dynamics and dependency of the closure time as a function of the gap size compared with the ones observed for larger gaps (Figs. 2*C* and 3*A*). This strikingly universal behavior is suggestive of a mechanism of purely physical origin. One such mechanism could be cell spreading based on an unspecific mechanical balance between cell-substrate adhesion and cortical tension (30). This mechanism has been shown to produce a linear dependence of spreading area with time. Moreover, it is consistent with a decrease of closure time with higher cell density because denser cells are more columnar and thus offer larger lateral area for cell spreading (Fig. 2*F* and Fig. S5).

Cell Crawling Drives the Closure of Large Gaps. By contrast, the closure time of large gaps (>20 μm) was not universal. Surprisingly, inhibition of either MLCK or ROCK had no significant effect in gap closure progression (Fig. 3*A* and Movies S4 and S5). RhoA has been described as an activator of myosin contraction required for purse-string closure, which is in turn regulated by MLCK and ROCK (9). Our findings thus suggest that the closure of large gaps is not driven by purse-string contraction. To ascertain this possibility in our closure model, we investigated actomyosin distribution at the gap edge. The presence per se of PDMS pillars for gap patterning did not trigger actin accumulation at the pillar periphery (Fig. S7 *A* and *B*). However, phalloidin staining immediately after pillar removal showed that actin accumulated in a continuous supracellular cable-like structure at the margins of the gap (Fig. S7 *C* and *D*). This surrounding actin cable was then disrupted as closure proceeded: the discontinuity of the actin cable was concomitant to the formation of cell protrusions, such as the extension of multiple lamellipodia into the gaps (Fig. 3 *B* and *C*). Moreover, according to confocal images in the *x*–*z* and *y*–*z* planes, it appeared that areas of actin accumulation localized at the lateral surface of cuboidal cells, whereas lamellipodial extension induced a flattening of the monolayer with a more diffuse and homogeneous actin distribution (Fig. S7 *E* and *F*). Staining of phospho-MLC as a marker for contractile myosin showed that active myosin colocalized with the actin cable immediately after pillar removal. However, as closure progressed, myosin in the cable accumulated only at the margins of major actin clustering (Fig. 3*C*). Previous results suggested that apoptotic cells release signals that favor the assembly of a continuous actomyosin cable all around the dying cell to promote the extrusion of the cell from the monolayer (31). Our findings showed that only an incomplete acto-myosin ring could form in the absence of cell injury. This suggests that death factors are required to develop a functional multicellular actomyosin cable.

In contrast to the inhibition of RhoA, the inhibition of Rac1 drastically slowed down the closure process of large gaps. Rac1 inhibition precluded the extension of lamellipodia and maintained a strong circularity of the gaps throughout closure (Fig. 2*B* and Movie S6). The larger the gaps, the more affected the closure was by Rac1 inhibition (Fig. 3*D*). Interestingly, Rac inhibition did not have such a slowing-down effect in damage-associated gaps, which progressed similarly to noninhibited damaged gaps (Fig. S2*D*) Taken together, our findings demonstrate a dominant role of cell crawling over purse-string closure in the absence of cell damage. This observation supports a recently proposed theoretical mechanical model for wound closure, in which crawling cells can close wounds without purse-string signaling, only because of their directed mechanical activity (32).

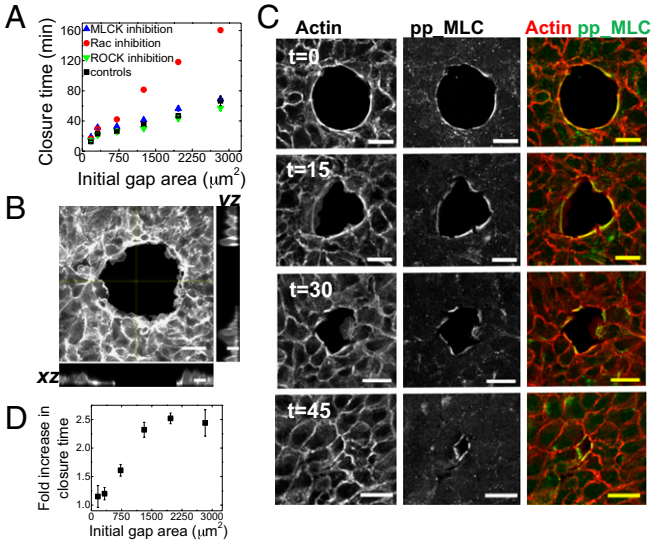

Fig. 3. Mechanism of gap closure: effect of inhibitors and actomyosin distribution. (*A*) Closure times of the different gap sizes in control conditions and subjected to drug treatments of the regulators (MLCK, ROCK, and Rac1 inhibition, for six gap sizes). Data points represent means, and error bars are SEs of seven analyzed gaps. (*B*) Z-stack projection and *x*–*z* and *y*–*z* orthogonal projections (sections from the yellow lines), after 30 min of closure progression Note that there is actin clustering at some cell edges and lamellipodia. (Scale bars, 25 μm in the z-projection, 5 μm in the orthogonal projections.) (*C*) Actin and phospho-MLC accumulate at the gap margin at *t* = 0 min but do not progress as a continuous ring as closure proceeds. (Scale bars, 20 μm.) (*D*) Fold increase in the closure time of Rac-inhibited cells with respect to control conditions for the six different gap sizes.

Influence of the Geometry of the Gaps. Because epithelial gap closure occurs in various geometrical conditions in vitro as well as in vivo, we studied the influence of curvature and shape of the gap on the closure process. We fabricated squared and ellipsoidal-like pillars (hereafter referred as ellipsoidal pillars) of two different sizes (Fig. 4*A*). Cells distributed randomly along the gap perimeter, with no preferential alignment of cells in areas of different curvature (Fig. S1 *F*–*K*). Live-cell microscopy showed that, regardless of the shape of the gaps, cells extended lamellipodia throughout closure (Fig. 4*C* and Movies S7 and S8) and that these lamellipodia were preferentially protruded along the edges with the lowest curvature. We then analyzed the closure time of squared and ellipsoidal gaps relative to circular ones. Except in the case of the smallest square analyzed, gaps of ellipsoidal and squared shape closed systematically faster than circular ones (Fig. 4*B*). This faster response might be due to the enhancement of lamellipodial activity in regions of low curvature. A physical model had previously reported that epithelial cells can sense and respond to different global geometric conditions by detecting the curvature of the epithelial edge at a multicellular level (33).

Much as in the case of circular gap experiments, actin and phospho-myosin accumulated preferentially at areas in which lamellipodia did not protrude, thus a supracellular cable was not continuous (Fig. 4 *D*–*F*). Hence, these results indicate that the behavior observed in the closure of circular gaps applies also to different gap geometries. This result is in good agreement with previous studies showing that large wounds (i.e., lower curvature) are preferentially Rac-dependent, whereas small ones (i.e., larger curvature) exhibit a purse-string mechanism (5, 6).

Collective Cell Movements by Cell–Cell Junctions and Myosin Action Provide Directional Clues. To further characterize cell rearrangements during gap closure, we analyzed the cells' shape and dynamics along the process. We tracked the trajectories of cells

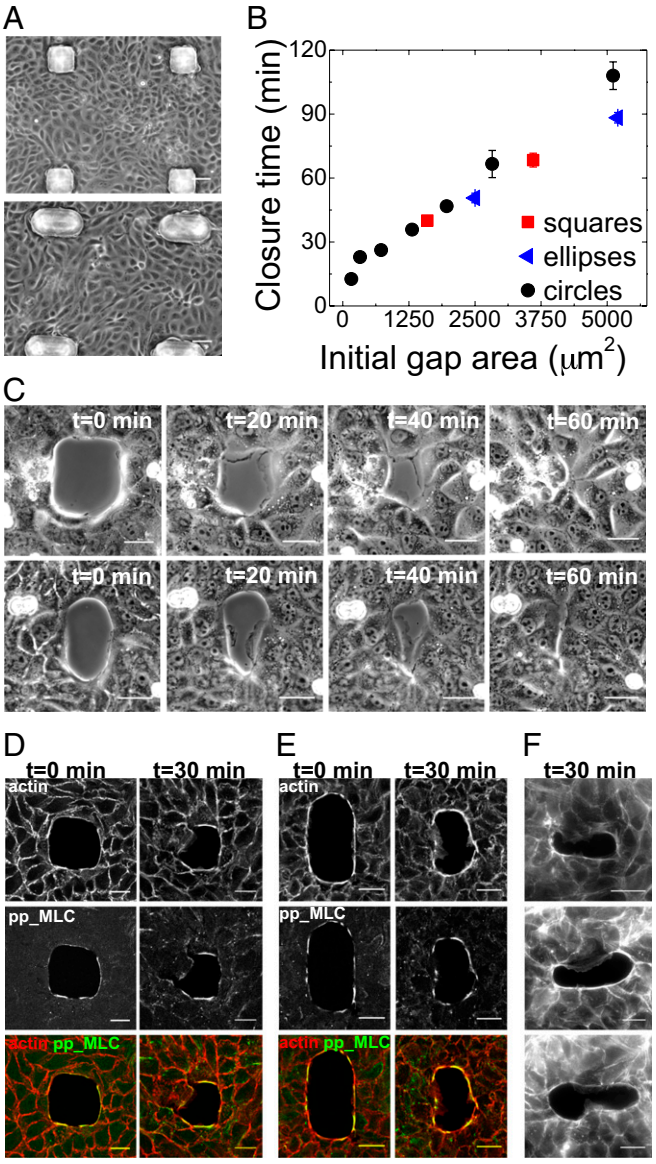

Fig. 4. Effect of geometry on gap closure. (*A*) Squared and ellipsoidal PDMS pillars surrounded by cells. (*B*) Comparison of the closure time of squared and ellipsoidal gaps with respect to circular gaps. (*C*) Sequence of phase-contrast micrographs showing the progression of the closure of a squared (*Top*) and ellipsoidal (*Bottom*) gap. (*D* and *E*) Actin (*Top*) and phospho-MLC (*Middle*) distribution in squared (*D*) and ellipsoidal (*E*) gaps for 2 different time points. (*Bottom*) Merged images. (*F*) Epifluorescence micrographs of actin distribution in the closure of ellipsoidal gaps 30 min after pillar removal. (Scale bars: 20 μm.)

during closure (Fig. S8 *A* and *B*). The first row of cells experienced directed motion toward the center of the gap and moved 98% ± 20% of the gap initial radius (Fig. S8 *A*, *B*, and *H*). Cells behind the leading edge showed progressively smaller and less persistent displacements (55% for the second row, 16% for outer cells). This result indicates that gap closure was mainly due to an active and directed process governed by cells at the leading edge and triggered by the presence of the free space, as previously described in the context of collective cell migration (7, 34).

Cells at the gap edge elongated along the direction of migration as closure progressed (Fig. S8*G*) and acquired a wedge-like morphology (Fig. 1*F*), further confirmed by the elongation of cell nuclei as an indicator of the cell polarization (Fig. S8*J*). At the closure time point, cells typically formed a rosette-like structure (Fig. 1*F* and Fig. S4*E*) that would be later dissolved through epithelial remodeling. Interestingly, this rosette-like structure has been observed in various situations related to the closure of gaps (8), apoptotic cell extrusion (31), cell delamination (35), embryonic healing (36), and in vitro wound healing (5).

To further understand the role of cell–cell communications in the gap closure process, we used an α-catenin knock-down MDCK cell line. As shown by Benjamin et al. (37), α-catenin knock-down MDCK cells display increased membrane dynamics together with higher migration rates but exhibit a lack of cadherin-mediated cell–cell adhesion. These cells, given that they do not form proper adherens junctions, could not support the formation of continuous multicellular cable surrounding the gap (15, 25) as well as a collective behavior mediated by cell–cell interactions. In our experimental model, they migrated independently of their position with respect to the gap edge, in an uncoordinated manner toward the gap center (Fig. S8 *C* and *D* and Movie S9). Thus, they displaced greater distances than WT MDCK cells owing to their lack of coordination (Fig. S8*H*). Gaps were still closed at a rate comparable to the WT MDCK cells (Fig. S8*I*). These findings demonstrate that gap closure can be accomplished without adherens junctions.

Although the absence of a continuous supracellular acto-myosin ring did not affect the closure kinetics, direct inhibition of myosin phosphorylation by blebbistatin caused a 1.7-fold increase in the closure time of large gaps (namely of 50 μm in diameter) (Fig. S8*I*). This observation suggests that myosin may contribute to gap closure through a mechanism that is independent of purse-string contraction. Cells treated with blebbistatin extended very broad lamellipodia with considerable ruffling activity (Movie S10). Compared with controls, cells moved longer distances, but their paths were not directed toward the center of the gap (Fig. S8 *E* and *F*). Moreover, the displacement magnitude was greater (approximately 150% displacement of the initial radius) and independent of the distance from the gap edge (Fig. S8*H*). Thus, the closure under blebbistatin treatment was achieved in an uncoordinated manner, resulting in a delay in the time of closure (Fig. S8*I*). Myosin IIA silencing or inhibition has previously been shown to cause increased membrane ruffling and migration speed in numerous cell types (38). Our findings show that this phenotype is not restricted to the single-cell level and suggest that the role of myosin IIA is not to drive collective cell motion but to guide it.

Conclusions

We have presented a unique approach to study gap closure in uninjured epithelia under well-defined experimental conditions. This provides a model for naturally occurring gaps in development, avoiding possible effects of cell death in gap closure. Such model experiments are also useful to discriminate between the different mechanisms proposed for epithelial gap closure (5, 6, 23). By using a microfabricated stencil with an array of pillars, gaps of precise size and shape can be patterned in parallel in an epithelial cell culture. Upon pillar removal, cells actively respond to the free space by extending lamellipodia and crawling into the gap.

Interestingly, small gaps (≤20 μm) show no response to the inhibition of myosin filament assembly or myosin contraction. Moreover, closure of such small areas is dependent on the cell density of the epithelium, because small gaps close faster in highly packed cultures. This evidence indicates that small gaps are closed by unspecific cell spreading. For gaps larger than 20 μm, the closure process is not altered when regulators of the purse-string contraction are inhibited, whereas disturbance of lamellipodial extension causes a drastic delay in closure. In addition, the intercellular actomyosin belt is lost during progression of closure, thus pointing out a pivotal role of cell crawling in the closure response.

To date, the cell crawling-mediated response has been mostly referred to wounds that could be considered infinitely large (6, 7, 39). We show here that even small gaps (of dozens of micrometers in diameter) are closed by means of lamellipodial

extension. The mere presence of free space has been proposed as the triggering mechanism for this response (7, 34).

In classic scratch-wound experiments, the purse-string mechanism has been found responsible for the closure of the wound. Purse-string has also been proposed for accounting for the extrusion of apoptotic cells (31), a process clearly related to death signaling, whereby the actomyosin cable formation is triggered through a caspase-mediated pathway (40). Thus, evidence suggests that cell damage inflicted during the process of wound production is promoting the purse-string mechanism by affecting the neighboring cells. In concordance with this hypothesis, we show here that in the absence of cell damage, purse-string is not the dominant mechanism, but the closure is mediated by a lamellipodial-driven crawling mechanism. In our model, the role of a supracellular actin belt is related to the coordination of the migrating cells toward the center of the gap, ensuring the proper directionality and persistence of their migration.

Interestingly, our results suggest that cells extending lamellipodia act as leader cells to close the gap. Indeed, it is known that protrusive lamellipodia are related to the mechanical probing of the substrate. On soft substrates, either we did not observe the formation of lamellipodia or they appear smaller and shorter in time. As a result, cells could not close the gap. The closure mechanism is thus associated with stabilization of protruding lamellipodia that help to generate stronger forces at the leading edge (28, 41). Finally, we show that squared and ellipsoidal gaps are closed faster than circular ones. Low curvature areas promote the protrusion of broad lamellipodia, but a continuous purse-string is not formed in square nor ellipsoidal gaps. Therefore, closure of noncircular epithelial gaps also seems to be primarily driven by lamellipodial-mediated cell crawling.

Materials and Methods

PDMS micropillars of different sizes and shapes were fabricated as previously described (41). Micropillar stencils were stuck to fibronectin-coated glass-bottom dishes. MDCK cells were plated and allowed to grow between the pillars until confluence. Gap closure was monitored with live-cell microscopy upon peeling off of the stencil, and image analysis was performed in ImageJ. Further details on the fabrication of substrates, inhibitors treatments, and immunofluorescence microscopy are found in *SI Materials and Methods*.

ACKNOWLEDGMENTS. We thank J. Le Digabel, Y. Toyama, F. Gallet, J.-M. Di Meglio, members of the Integrative Cell and Tissue Dynamics Laboratory at IBEC, and members of the Mechanobiology Institute (National University of Singapore) for fruitful discussions; A. Richert for cell culture protocols; W. J. Nelson (Stanford University) for kindly providing the α-catenin knockdown MDCK cell line; and the microfabrication core of MBI. Financial support was received from the Association pour la Recherche sur le Cancer, the Association Française Contre la Myopathie, the Agence Nationale de la Recherche [Programme Blanc 2010 (MECANOCAD)], Grant BFU2009-07595 from the Spanish Ministry for Science and Innovation, Grant Agreement 242993 from the European Research Council, and MBI. The research was conducted in the scope of the International Associated Laboratory Cell Adhesion France-Singapore. E.A. receives financial support from the Fondation pour la Recherche Médicale.

1. Martin P, Parkhurst SM (2004) Parallels between tissue repair and embryo morphogenesis. *Development* 131:3021–3034.
2. Jacinto A, Martinez-Arias A, Martin P (2001) Mechanisms of epithelial fusion and repair. *Nat Cell Biol* 3:E117–E123.
3. Watson AJ, et al. (2005) Epithelial barrier function in vivo is sustained despite gaps in epithelial layers. *Gastroenterology* 129:902–912.
4. Bement WM, Mandato CA, Kirsch MN (1999) Wound-induced assembly and closure of an actomyosin purse string in *Xenopus* oocytes. *Curr Biol* 9:579–587.
5. Tamada M, Perez TD, Nelson WJ, Sheetz MP (2007) Two distinct modes of myosin assembly and dynamics during epithelial wound closure. *J Cell Biol* 176:27–33.
6. Fenteany G, Janmey PA, Stossel TP (2000) Signaling pathways and cell mechanics involved in wound closure by epithelial cell sheets. *Curr Biol* 10:831–838.
7. Poujade M, et al. (2007) Collective migration of an epithelial monolayer in response to a model wound. *Proc Natl Acad Sci USA* 104:15988–15993.
8. Bement WM, Forscher P, Mooseker MS (1993) A novel cytoskeletal structure involved in purse string wound closure and cell polarity maintenance. *J Cell Biol* 121:565–578.
9. Nobes CD, Hall A (1995) Rho, rac, and cdc42 GTPases regulate the assembly of multimolecular focal complexes associated with actin stress fibers, lamellipodia, and filopodia. *Cell* 81:53–62.
10. Kim J-H, Dooling LJ, Asthagiri AR (2010) Intercellular mechanotransduction during multicellular morphodynamics. *J R Soc Interface* 7(Suppl 3):S341–S350.
11. Salbreux G, Prost J, Joanny JF (2009) Hydrodynamics of cellular cortical flows and the formation of contractile rings. *Phys Rev Lett* 103:058102.
12. Trepat X, et al. (2009) Physical forces during collective cell migration. *Nat Phys* 5: 426–430.
13. Desai LP, Aryal AM, Ceacareanu B, Hassid A, Waters CM (2004) RhoA and Rac1 are both required for efficient wound closure of airway epithelial cells. *Am J Physiol Lung Cell Mol Physiol* 287:L1134–L1144.
14. Russo JM, et al. (2005) Distinct temporal-spatial roles for rho kinase and myosin light chain kinase in epithelial purse-string wound closure. *Gastroenterology* 128: 987–1001.
15. Danjo Y, Gipson IK (1998) Actin 'purse string' filaments are anchored by E-cadherin-mediated adherens junctions at the leading edge of the epithelial wound, providing coordinated cell movement. *J Cell Sci* 111:3323–3332.
16. Florian P, Schöneberg T, Schulzke JD, Fromm M, Gitter AH (2002) Single-cell epithelial defects close rapidly by an actinomyosin purse string mechanism with functional tight junctions. *J Physiol* 545:485–499.
17. Todaro GJ, Lazar GK, Green H (1965) The initiation of cell division in a contact-inhibited mammalian cell line. *J Cell Physiol* 66:325–333.
18. Klepeis VE, Cornell-Bell A, Trinkaus-Randall V (2001) Growth factors but not gap junctions play a role in injury-induced Ca2+ waves in epithelial cells. *J Cell Sci* 114: 4185–4195.
19. Block ER, Matela AR, SundarRaj N, Iszkula ER, Klarlund JK (2004) Wounding induces motility in sheets of corneal epithelial cells through loss of spatial constraints: Role of heparin-binding epidermal growth factor-like growth factor signaling. *J Biol Chem* 279:24307–24312.
20. McNeil PL (2002) Repairing a torn cell surface: Make way, lysosomes to the rescue. *J Cell Sci* 115:873–879.
21. Woolley K, Martin P (2000) Conserved mechanisms of repair: From damaged single cells to wounds in multicellular tissues. *Bioessays* 22:911–919.
22. Brock J, Midwinter K, Lewis J, Martin P (1996) Healing of incisional wounds in the embryonic chick wing bud: Characterization of the actin purse-string and demonstration of a requirement for Rho activation. *J Cell Biol* 135:1097–1107.
23. Garcia-Fernandez B, Campos I, Geiger J, Santos AC, Jacinto A (2009) Epithelial resealing. *Int J Dev Biol* 53:1549–1556.
24. Reffay M, et al. (2011) Orientation and polarity in collectively migrating cell structures: Statics and dynamics. *Biophys J* 100:2566–2575.
25. Abreu-Blanco MT, Verboon JM, Parkhurst SM (2011) Cell wound repair in *Drosophila* occurs through three distinct phases of membrane and cytoskeletal remodeling. *J Cell Biol* 193:455–464.
26. Nicolás FJ, Lehmann K, Warne PH, Hill CS, Downward J (2003) Epithelial to mesenchymal transition in Madin-Darby canine kidney cells is accompanied by down-regulation of Smad3 expression, leading to resistance to transforming growth factor-beta-induced growth arrest. *J Biol Chem* 278:3251–3256.
27. Pelham RJ, Jr., Wang YL (1998) Cell locomotion and focal adhesions are regulated by the mechanical properties of the substrate. *Biol Bull* 194:348–349, discussion 349–350.
28. Giannone G, et al. (2004) Periodic lamellipodial contractions correlate with rearward actin waves. *Cell* 116:431–443.
29. Saez A, et al. (2010) Traction forces exerted by epithelial cell sheets. *J Phys Condens Matter* 22:194119.
30. Cuvelier D, et al. (2007) The universal dynamics of cell spreading. *Curr Biol* 17:694–699.
31. Rosenblatt J, Raff MC, Cramer LP (2001) An epithelial cell destined for apoptosis signals its neighbors to extrude it by an actin- and myosin-dependent mechanism. *Curr Biol* 11:1847–1857.
32. Lee P, Wolgemuth CW (2011) Crawling cells can close wounds without purse strings or signaling. *PLoS Comput Biol* 7:e1002007.
33. Mark S, et al. (2010) Physical model of the dynamic instability in an expanding cell culture. *Biophys J* 98:361–370.
34. Nikolić DL, Boettiger AN, Bar-Sagi D, Carbeck JD, Shvartsman SY (2006) Role of boundary conditions in an experimental model of epithelial wound healing. *Am J Physiol Cell Physiol* 291:C68–C75.
35. Muliyil S, Krishnakumar P, Narasimha M (2011) Spatial, temporal and molecular hierarchies in the link between death, delamination and dorsal closure. *Development* 138:3043–3054.
36. Meghana C, et al. (2011) Integrin adhesion drives the emergent polarization of active cytoskeletal stresses to pattern cell delamination. *Proc Natl Acad Sci USA* 108: 9107–9112.
37. Benjamin JM, et al. (2010) AlphaE-catenin regulates actin dynamics independently of cadherin-mediated cell-cell adhesion. *J Cell Biol* 189:339–352.
38. Even-Ram S, et al. (2007) Myosin IIA regulates cell motility and actomyosin-microtubule crosstalk. *Nat Cell Biol* 9:299–309.
39. Omelchenko T, Vasiliev JM, Gelfand IM, Feder HH, Bonder EM (2003) Rho-dependent formation of epithelial "leader" cells during wound healing. *Proc Natl Acad Sci USA* 100:10788–10793.
40. Andrade D, Rosenblatt J (2011) Apoptotic regulation of epithelial cellular extrusion. *Apoptosis* 16:491–501.
41. du Roure O, et al. (2005) Force mapping in epithelial cell migration. *Proc Natl Acad Sci USA* 102:2390–2395.